Peroxide-Dependent Formation of a Covalent Link between Trp51 and the Heme in Cytochrome *c* Peroxidase[†]

Zoi Pipirou,[‡] Victor Guallar,[§] Jaswir Basran,[||] Clive L. Metcalfe,[‡] Emma J. Murphy,[‡] Andrew R. Bottrill,[⊥] Sharad C. Mistry,[⊥] and Emma Lloyd Raven*[,‡]

Department of Chemistry, Henry Wellcome Building, University of Leicester, University Road, Leicester LE1 7RH, England, ICREA, Life Science Department, Barcelona Supercomputing Center, Jordi Girona 29, 08034 Barcelona, Spain, Department of Biochemistry, Henry Wellcome Building, University of Leicester, Lancaster Road, Leicester LE1 9HN, England, and Protein and Nucleic Acid Chemistry Laboratory, Hodgkin Building, University of Leicester, Lancaster Road, Leicester LE1 9HN, England

Received December 2, 2008; Revised Manuscript Received February 26, 2009

ABSTRACT: Ascorbate peroxidase (APX), cytochrome *c* peroxidase (C*c*P), and the catalase−peroxidases (KatG) share very similar active site structures and are distinguished from other peroxidases by the presence of a distal tryptophan residue. In KatG, this distal tryptophan forms a covalent link to an adjacent tyrosine residue, which in turn links to a methionine residue. We have previously shown [Pipirou, Z. et al. (2007) *Biochemistry 46*, 2174−2180] that reaction of APX with peroxide leads, over long time scales, to formation of a covalent link with the distal tryptophan (Trp41) in a mechanism that proceeds through initial formation of a compound I species bearing a porphyrin π-cation radical followed by radical formation on Trp41, as implicated in the KatG enzymes. Formation of such a covalent link in C*c*P has never been reported, and we proposed that this could be because compound I in C*c*P uses Trp191 instead of a porphyrin π-cation radical. To test this, we have examined the reactivity of the W191F variant of C*c*P with H_2O_2, in which formation of a porphyrin π-cation radical occurs. We show, using electronic spectroscopy, HPLC, and mass spectroscopy, that in W191F partial formation of a covalent link from Trp51 to the heme is observed, as in APX. Radical formation on Trp51, as seen for KatG and APX, is implicated; this is supported by QM/MM calculations. Collectively, the data show that all three members of the class I heme peroxidases can support radical formation on the distal tryptophan and that the reactivity of this radical can be controlled either by the protein structure or by the nature of the compound I intermediate.

The class I heme peroxidase enzymes, the most prominent members of which are cytochrome *c* peroxidase (C*c*P), ascorbate peroxidase (APX),[1] and the bifunctional catalase−peroxidases (KatG), are distinguished from other heme peroxidases by the presence of a distal tryptophan residue in place of the more usual phenylalanine residue and a second active site tryptophan adjacent to the proximal histidine ligand (Figure 1). A key distinguishing feature of the catalase−peroxidase enzymes is that they contain a covalent cross-link between the distal tryptophan and adjacent tyrosine and methionine residues (*1*−*5*), Figure 1a. The functional role of this covalent link is not clearly established, but the fact that it is not observed in the monofunctional peroxidases (APX and C*c*P, Figure 1b,c) suggests that it might be connected with catalatic activity in KatGs (*6*−*8*). The mechanism of formation of the link in KatG is proposed (*4, 9*) to involve initial reaction with peroxide to form a compound I intermediate (containing a ferryl heme and a porphyrin π-cation radical) followed by formation of both tryptophan and tyrosine radicals through a normal oxidative peroxidase mechanism. A second cycle of reaction with H_2O_2 is then proposed for formation of the tyrosine−methionine link.

Recently, we have demonstrated (*10*) that covalent linking of Trp41 to the heme group in ascorbate peroxidase can occur under noncatalytic conditions on exposure of the enzyme to peroxide, and a reaction mechanism involving initial formation of a porphyrin π-cation radical followed by radical formation at Trp41 has been implicated. We interpreted this to mean that radical formation at the distal tryptophan residue is not an exclusive feature of the KatG enzymes and that this radical intermediate is accessible in other related peroxidases. If this is the case, it follows that the route by which APX and C*c*P legislate against formation of this link is largely structural (i.e., the absence of tyrosine or methionine residues, Figure 1b,c) rather than an intrinsic inability to form a tryptophan radical.

In preliminary experiments on C*c*P (*10*), no evidence for formation of an analogous cross-link of the heme to Trp51

[†] This work was supported by grants from The Leverhulme Trust, BBSRC (Grants BB/C001184/1 (to E.R./PCEM), BBS/S/A/2004/12421 (studentship to E.J.M.) and IIP0206/009 (fellowship to E.R.)), EPSRC (studentship to Z.P.), and the Spanish Ministry of Education (Grant CTQ2007-62122 to V.G.).

* To whom correspondence should be addressed. Telephone: +44 (0)116 2297047. Fax: +44 (0)116 252 3789. E-mail: emma.raven@le.ac.uk.

[‡] Department of Chemistry, University of Leicester.

[§] ICREA, Barcelona Supercomputing Center.

[||] Department of Biochemistry, University of Leicester.

[⊥] Protein and Nucleic Acid Chemistry Laboratory, University of Leicester.

[1] Abbreviations: APX, ascorbate peroxidase; rsAPX, recombinant soybean cytosolic ascorbate peroxidase; C*c*P, cytochrome *c* peroxidase; KatG, catalase−peroxidase; *mt*KatG, *Mycobacterium tuberculosis* catalase−peroxidase; QM/MM, quantum mechanics/molecular mechanics.

10.1021/bi802210g CCC: $40.75
Published on Web 02/27/2009

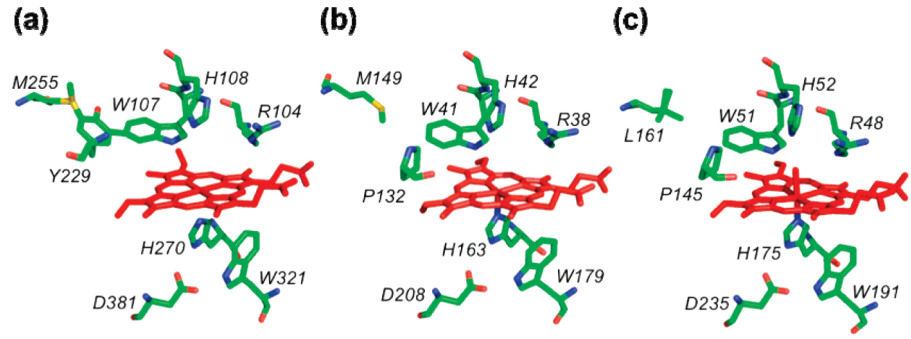

FIGURE 1: Structures of (a) *mt*KatG (PDB 1SJ2), (b) APX (1OAG), and (c) C*c*P (2CYP), showing the covalent links in *mt*KatG and the equivalent residues in APX and C*c*P.

was observed. We proposed that this was because C*c*P immediately diverts oxidizing equivalents to Trp191 as the immediate product of H_2O_2 oxidation without detectable formation of a porphyrin π-cation radical (*11*−*13*), which is thought to be an obligate intermediate of the mechanism for heme−protein cross-linking (as described above). To test this hypothesis in further detail, we have examined the reactivity of the W191F variant of C*c*P, in which, in contrast to CcP, an oxyferryl porphyrin π-cation radical intermediate is formed on reaction with H_2O_2 (*14, 15*). HPLC and mass spectrometry data for this variant show that partial formation of a covalently linked product indeed occurs in the W191F variant, as seen for APX, and we propose that this is related to the ability of the W191F variant to form a compound I intermediate bearing a porphyrin π-cation radical instead of the more usual Trp191 cation radical in C*c*P.

EXPERIMENTAL PROCEDURES

Materials. All buffers were of the highest analytical grade (99% + purity) and used without further purification. Sinapinic acid and α-cyano-4-hydroxycinnamic acid were purchased from Fluka. All other chemicals were purchased from Sigma. Water was purified by an Elga purelab purification system, and all buffers were filtered (0.2 μm) prior to use. Hydrogen peroxide solutions were freshly prepared by dilution of a 30% (v/v) solution (BDH); exact concentrations were determined using the published absorption coefficient ($\varepsilon_{240} = 39.4\ M^{-1}\ cm^{-1}$) (*16*). All molecular biology kits and enzymes were used according to manufacturer's protocols.

Protein Expression and Purification. Wild-type C*c*P and W191F were prepared and isolated with modifications to published procedures (*17*), as described previously (*18*). The C*c*P(MKT) gene was a generous gift from Professor Grant Mauk (University of British Columbia). Purified samples of wild-type C*c*P and W191F showed wavelength maxima at 409, 506, 544^{sh}, 589^{sh}, and 647 nm and 409, 504, 544^{sh}, 589^{sh}, and 645 nm (150 mM potassium phosphate, pH 6.0), respectively. Enzyme concentrations for C*c*P and W191F were determined using absorption coefficients of $\varepsilon_{409} = 95$ (*19*) and 102 $mM^{-1}cm^{-1}$, respectively.

Electronic Absorption Spectroscopy. Spectra were collected using a Perkin-Elmer Lambda 35 or 40 spectrophotometer linked to a PC workstation running UV-Winlab software. Reactions of C*c*P and W191F with H_2O_2 were carried out at pH 7.0 in a 10 mM potassium phosphate buffer with sufficient KNO_3 to adjust the ionic strength to 0.1 M.

Transient-State Kinetics. Transient kinetics were performed using an Applied Photophysics SX.18MV-R microvolume stopped-flow spectrophotometer fitted with a Neslab RTE200 circulating water bath. Time-dependent spectra (in 100 mM potassium phosphate, pH 7.0, 25.0 °C) were performed by multiple wavelength stopped-flow spectroscopy using a photodiode array detector and X-SCAN software (Applied Photophysics) by reacting W191F (3.5 μM) with 1 or 5 equiv of H_2O_2 (3.5 or 17.5 μM), and the reaction was followed over time scales ranging from 3 ms to 1 s.

Characterization of Protein Fragments. HPLC analysis of protein and peptide samples and tryptic digestions were carried out according to published protocols (*10*). MALDI-TOF analyses of protein and peptide samples and MS/MS analysis of peptide samples were carried out according to published protocols (*10*).

QM/MM Methods and System Preparation. QM/MM methods join together QM and MM representations of different sectors of a complex system (*20, 21*). The models for compound I of C*c*P were extracted from the structure (PDB code 2CYP). The closest crystallographic water molecule to the iron center was used to model the oxo ligand. The W191F mutation was performed by side chain replacement followed by four iterations of side chain sampling plus minimization of a region within 6 Å of Trp191. Preparation of both wild-type C*c*P and W191F included soaking the protein in a box of pre-equilibrated water molecules followed by 100 ps of NPT molecular dynamics at 300 K using periodic boundary conditions. For the molecular dynamics as well as for the MM part of the QM/MM calculations, we used the OPLS-AA (*22*) force field and the Impact program (*23*). For the molecular dynamics, the iron plus all its first coordination shell atoms (a total of seven atoms) were constrained. For the QM/MM minimizations, only a 10 Å layer of water molecules surrounding the proteins was used. The quantum region includes the heme, His163, the oxygen ligand, Trp51, and Trp191 (or Phe191). In all QM/MM optimizations, the last layer of oxygen atoms from the explicit water solvent was constrained. QM/MM calculations were performed with the Qsite program (*24*). Geometry optimizations used unrestricted DFT (B3LYP) in combination with the LACVP* basis sets.

RESULTS

Reaction of Wild-Type CcP with Hydrogen Peroxide and HPLC Analyses. Purified samples of C*c*P showed wavelength maxima at 409 ($\varepsilon = 95\ mM^{-1}\ cm^{-1}$), 506, 544^{sh}, 589^{sh}, and 647 nm (100 mM potassium phosphate, pH 6.0), as reported previously (*25*). In order to examine whether wild-type C*c*P exhibits similar behavior to wild-type APX (i.e., whether it

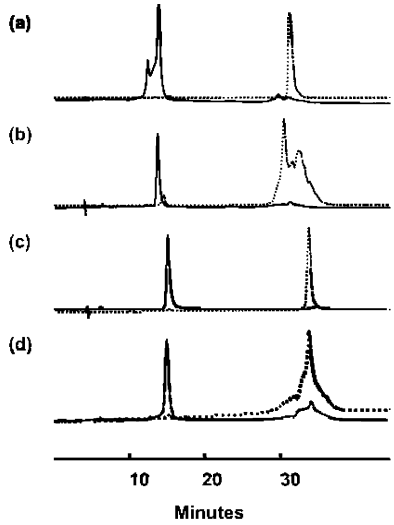

FIGURE 2: HPLC analyses of C*c*P and W191F before and after reaction with 6 equiv of H_2O_2 (150 mM potassium phosphate, pH 6.0), monitored at 398 nm (solid line) and 215 nm (dotted line): (a) C*c*P before reaction with H_2O_2; (b) C*c*P after reaction with H_2O_2; (c) W191F before reaction with H_2O_2; (d) W191F after reaction with H_2O_2.

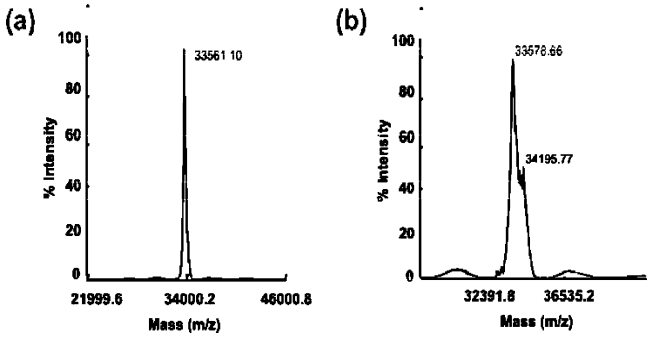

FIGURE 3: MALDI-TOF mass spectrum of W191F before (a) and after (b) reaction with 6 equiv of H_2O_2.

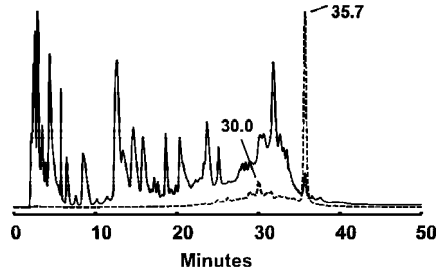

FIGURE 4: HPLC analyses of a tryptically digested sample of W191F after reaction with H_2O_2, monitored at 215 nm (solid line) and 398 nm (dotted line). Elution times of heme-containing peptides (30.0 min), as well as free heme (35.7 min), are indicated.

forms a link from Trp51 to the heme on reaction with H_2O_2), we reacted C*c*P with 6 equiv of H_2O_2 at pH 7 and followed the reaction using UV−visible spectroscopy, as reported previously for wild-type APX (*10*). (The choice of stoichiometry ([protein]/[H_2O_2]) is a balance between obtaining acceptable yields of covalently linked product and avoiding nonspecific heme bleaching or degradation at high concentrations of H_2O_2, especially over long time scales. We used 6 equiv of H_2O_2 to be consistent with our previous work on APX (*10*) in which we found that higher concentrations of peroxide lead to heme degradation.) Reaction of C*c*P with H_2O_2 resulted in clean formation of compound I (λ_{max} (nm) = 420, 530, and 561) as expected (*26, 27*), which decays over ~2 h to compound II (λ_{max} (nm) = 413, 532 and 569^{sh}, data not shown). HPLC analysis of protein samples was carried out at both 398 nm (reporting on the heme content) and 215 nm (reporting on the protein) before (Figure 2a) and after (Figure 2b) treatment of C*c*P with hydrogen peroxide under the same conditions as those used for wild-type APX (*10*). There is no coelution of the heme with the protein, Figure 2b.

Reaction of W191F with Hydrogen Peroxide and HPLC Analyses. Reaction of W191F is known (*14, 15, 28*) to lead to formation of a transient compound I intermediate that has spectroscopic properties consistent with those expected for a porphyrin π-cation radical. We have reported (*18*) similar behavior: W191F exhibits spectroscopic changes on reaction with H_2O_2 consistent with formation of a transient porphyrin π-cation radical (λ_{max} (nm) = 412, 543, and 656). This compound I decays to a species (λ_{max} (nm) = 423, 535, and 565) that is consistent with an oxy-ferryl heme and a protein radical (*29*). Experiments using a pyridine hemochromagen assay suggested that, on reaction with H_2O_2, the heme group in W191F becomes covalently attached to the protein over longer time scales (~2 h). This was confirmed qualitatively in two ways as described below.

First, HPLC analysis of the product of the reaction of W191F with H_2O_2 (prepared with addition of 6 equiv of H_2O_2) showed that the protein (monitored at 215 nm) and some proportion of the heme (monitored at 398 nm) coelute at 33 min (Figure 2d); this is in direct contrast to the HPLC profile of W191F that has not been treated with H_2O_2, in which the heme (13 min) and the protein (33 min) do not coelute (Figure 2c). Coelution of the heme and the protein fragments is a clear indication of covalent heme attachment and has been used previously to identify covalently linked heme in various other heme proteins, including APX (*30*−*36*).

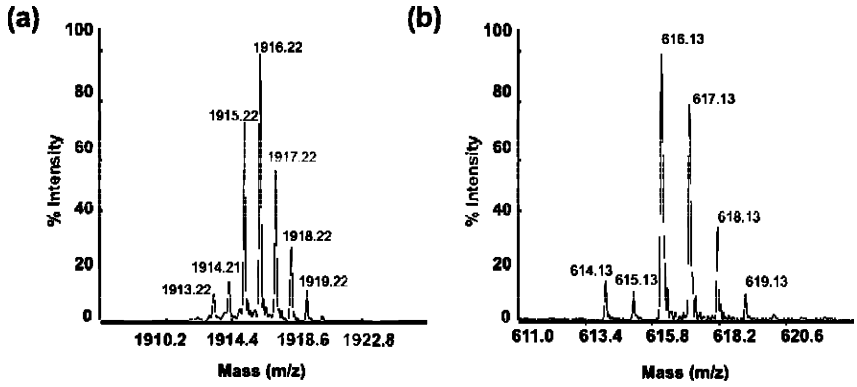

FIGURE 5: MALDI-TOF mass spectrum of (a) the HPLC-purified heme-containing fragment obtained after reaction of W191F with H_2O_2 and (b) heme, showing the characteristic heme isotope pattern as reported previously (*37*).

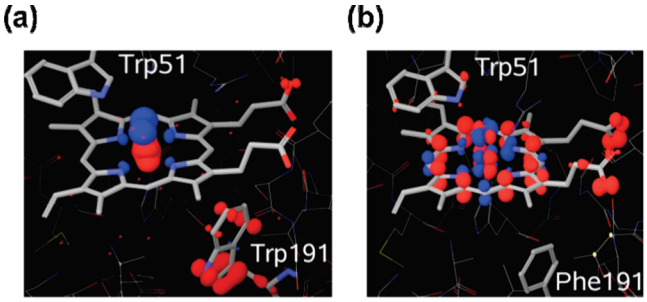

FIGURE 6: Doublet state spin densities for the compound I intermediate of (a) wild-type and (b) W191F. All three unpaired electrons are shown. Positive (blue) and negative (red) spin densities are indicated. The heme, Trp51, and Trp(Phe)191 are indicated.

We note, however, that the yield of covalently linked product (estimated from peak areas in the HPLC chromatograms) was overall lower for C*c*P than previously observed for APX (*10*) (see Discussion).

Second, the MALDI-TOF mass spectrum of W191F before treatment with H_2O_2 showed a mass of 33561.10 Da (Figure 3a), which corresponds closely to the predicted mass (33554.4 Da) of the apoprotein and is consistent with noncovalent attachment of the heme (as found in APX). After treatment with H_2O_2, two peaks were observed in the MALDI-TOF spectrum, Figure 3b. The first is at 33578.66 Da[2] which is consistent with the mass of the apoprotein (as above). The second peak is at 34195.77 Da, which corresponds to a mass increase of 617 Da over the apoprotein, and is consistent with covalent attachment of the heme (616 Da) to the protein. Tryptic digestion of the product of the reaction of W191F with H_2O_2 was carried out, and HPLC was used to isolate the heme-containing peptide fragments (i.e., showing both heme and protein absorbance) from the resulting peptide mixture (Figure 4). The MALDI-TOF mass spectrum of the product eluting at 35.7 min gave a mass of 616 Da (Figure 5b), corresponding to free heme, as reported previously for APX (*10, 37*). MALDI-TOF mass spectrometry of the peptide fragment eluting at 30.0 min gave a mass of 1915.22 Da, which is 2 Da lower than the calculated mass of 1917 Da expected for the $L^{49}A\mathbf{W}^{51}HTSGTWDK^{59}$ peptide fragment containing heme covalently bound to Trp51[3] (Figure 5a). Further evidence for heme incorporation into this peptide fragment came from the characteristic heme isotope pattern (Figure 5a). As reported previously (*37*), iron exhibits a distinct isotope pattern in the mass spectrum when incorporated into protoporphyrin IX (Figure 5b). The fact that the peptide with mass of 1915.22 Da (Figure 5a) exhibits similar isotope pattern as heme (Figure 5b) (*37*) is further confirmation that it derives from a heme-containing peptide.

QM/MM Calculations. QM/MM methods (*38*) provide a useful means of assessing spin distribution in heme-containing systems (*39*−*43*). Accordingly, we have mapped the spin density for the compound I intermediate for both wild-type C*c*P and W191F; Figure 6 shows the spin density obtained in the doublet spin state. As shown previously, both doublet and quartet spin states are degenerate, showing almost identical spin density (*39, 42, 44*). For the wild-type protein, Figure 6a, the three unpaired electrons are localized on the iron-oxo moiety and on Trp191. For W191F, Figure 6b, there is a shift of the spin density for the "third" unpaired electron from Trp191 to the porphyrin, which is in agreement with the experimental observations.[4] For W191F, we also observe a small amount of spin density on Trp51, Figure 6b. Single point QM/MM calculations, to check the dependency of this

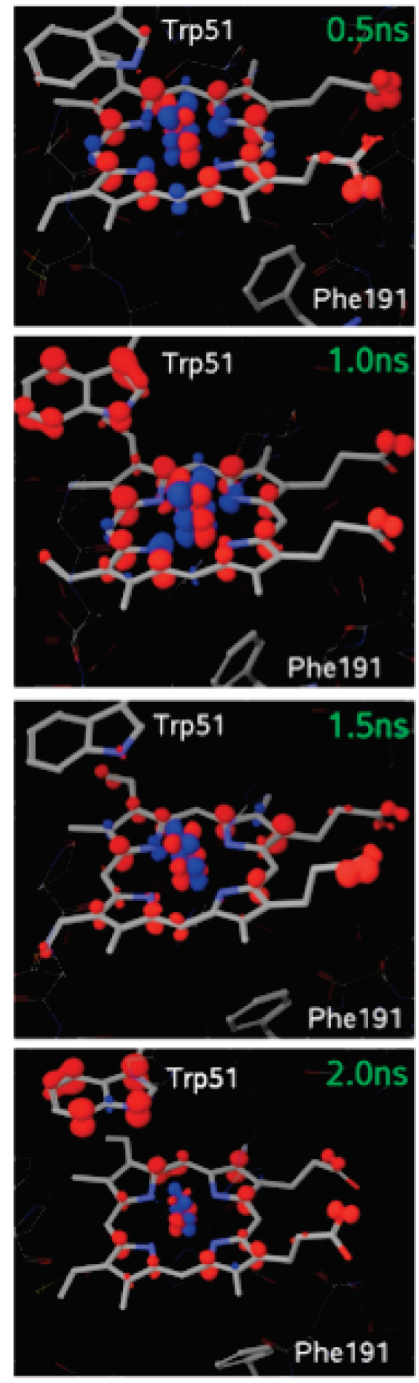

FIGURE 7: Evolution of the doublet state spin density for the W191F mutant along 2 ns of molecular dynamics. Positive and negative spin densities are depicted in blue and red, respectively. The heme, Trp51, and Trp(Phe)191 are indicated.

[2] The mass increase of +17.6 indicates possible oxidation (e.g., sulfoxide formation at methionine).

[3] However, in this case there was no additional mass to indicate that addition of an extra hydroxyl group to the heme-containing fragment had occurred, as previously seen for APX (*10*).

[4] We also observe a larger component of the spin density on the propionate groups, possibly as a result of a less effective screening for the propionates due to larger oscillations in the vicinity of these groups as a consequence of the mutation (*40*).

Scheme 1: Proposed Mechanism for Formation of a Covalent Link between Trp51 and the Heme Group in W191F Variant of C*c*P[a]

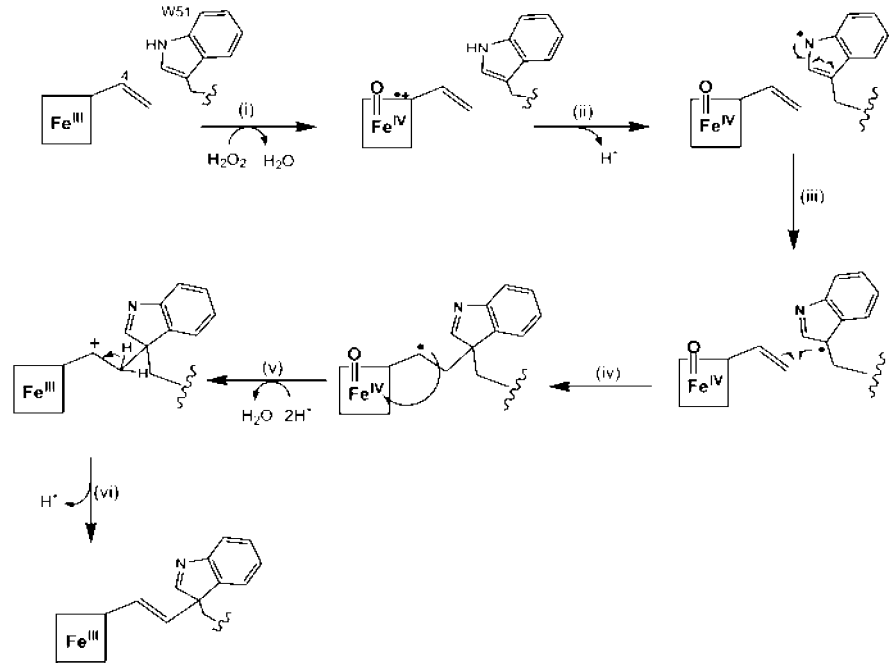

[a] Steps i−vi are described in the Discussion.

Trp51 spin density on protein fluctuations (*45, 46*), showed four intermediate states, at 0.5, 1.0, 1.5, and 2.0 ns, Figure 7, which show fluctuations in spin density between the porphyrin ring and Trp51.

DISCUSSION

The catalase peroxidases are distinguished from other class I peroxidase enzymes by the fact that their distal tryptophan is involved in a covalent tryptophan−tyrosine−methionine cross-link. The proposed (*4, 9*) mechanism for formation of this cross-link involves radical formation on Trp107. Although both APX and C*c*P contain the same distal tryptophan residue (Figure 1), no such cross-link has been observed in either of these enzymes. We have previously presented evidence that was consistent with radical formation on the equivalent distal tryptophan, Trp41, in APX. Hence, over long time scales (∼2 h) and under conditions where no substrate was present to quickly regenerate the ferric form, we observed covalent attachment of Trp41 to the heme (*10*). We proposed a mechanism that involved initial formation of a porphyrin π-cation radical followed by formation of a protein radical on Trp41. In this case, the fate of the supposed tryptophan radical is different from that in the catalase−peroxidase enzymes, because in APX there is no suitable active residue nearby with which it might react; instead, it reacts with the heme. By implication, and in view of the close structural similarity, we suggested that radical formation on the distal tryptophan might be a common feature across members of the class I peroxidase family. Consequently, the absence of a tryptophan−tyrosine−methionine cross-link in APX and C*c*P could be assigned to the absence of suitable residues adjacent to the distal tryptophan (Figure 1).

The aim of this work was to test this proposal further, with parallel experiments on C*c*P. C*c*P is unique among the class I peroxidases in that it immediately diverts oxidizing equivalents to a protein radical (Trp191) as the immediate product of H_2O_2 oxidation, without observable formation of a porphyrin π-cation radical. Since formation of the covalent link in the catalase peroxidases is thought to require a porphyrin π-cation intermediate (*4, 9*) and since APX forms the same porphyrin π-cation radical, we reasoned (*10*) that the absence of a corresponding heme−tryptophan link in C*c*P might be related to the identity of the compound I species (since in C*c*P a porphyrin π-cation radical is not observed, although it might form fleetingly, and compound I exists as a stable protein radical).[5] The W191F variant provides a convenient means of assessing this, since in this case formation of a radical at Trp191 is not possible and a transient porphyrin π-cation radical is observed instead (*14*).

Although the cross-linking reactions are substoichiometric, our HPLC analyses show that following exposure of W191F to 6 equiv of H_2O_2 the protein and some proportion of the heme coelute and that a peptide containing Trp51 can be isolated. This fragment was shown by mass spectrometry to be covalently attached to heme. We propose a similar mechanism for formation of the Trp51−heme link in W191F as that proposed previously (*10*) for the same link in APX (Scheme 1). In this mechanism, initial formation (step i) of a transient compound I intermediate, as observed by stopped flow, is followed by oxidation and deprotonation of Trp51 (step ii) and addition of the Trp51 radical across the 4-vinyl

[5] Timescales might be important here, so that the stability of the porphyrin π-cation radical might determine whether or not a cross-link is feasible. For KatG, a porphyrin π-cation radical is stable enough to be observed, but it has been shown that formation of a protein radical at Trp321 (equivalent to Trp191 in C*c*P) occurs subsequently (*54*). In wild-type C*c*P, a porphyrin π-cation radical has never been observed but might well be formed prior to formation of a radical in Trp191. We presume that if a porphyrin π-cation radical exists for C*c*P it is present much too fleetingly to be productive in terms of possible cross-linking mechanisms (unlike KatG).

group of the heme (steps iii and iv). Subsequent reduction of the ferryl group and release of H_2O (step v) leads to formation of a carbocation, and deprotonation at this position (instead of addition of a H_2O molecule, as proposed for APX (*10*)) as the final step (step vi) gives a product that is consistent with the mass spectrometry data.

A key element of the proposed mechanism is that formation of a porphyrin π-cation radical is followed by radical formation at the distal tryptophan for both APX and C*c*P. This proposal is supported by the QM/MM data for W191F, which show transient spin density on Trp51. Radical formation at numerous other sites is also possible in C*c*P, however (see, for example, refs *47*−*51*), which will decrease the percentage of heme that links covalently to Trp51. In fact, two populations of radical product for W191F have been reported (*50*): one of these leads to protein dimerization (through tyrosine residues) and our data would account for the other (radical formation on Trp51). Our work does not unambiguously establish Trp51 as a site of radical formation in W191F, but the proposed mechanism is consistent with other suggestions in the literature in which formation of a radical at this site has been implicated (*52*). In fact, Poulos and co-workers (*53*) have demonstrated peroxide-dependent formation of a Trp51−Tyr52 link in the H52Y variant of C*c*P: formation of this link is proposed to involve radical formation on Trp51 and Tyr52 in a mechanism that is analogous to that proposed for KatG (*4, 9*), which lends further support to our proposal (*10*) that this group of class I peroxidases share common reaction mechanisms and that radical formation at the distal tryptophan residue is more widely accessible than was previously realized.

ACKNOWLEDGMENT

We are grateful to Ann English for helpful discussions and Grant Mauk (University of British Columbia) for the C*c*P expression vector.

REFERENCES

1. Jakopitsch, C., Kolarich, D., Petutschnig, G., Furtmuller, P. G., and Obinger, C. (2003) Distal side tryptophan, tyrosine and methionine in catalase-peroxidases are covalently linked in solution. *FEBS Lett. 552*, 135–140.
2. Yamada, Y., Fujiwara, T., Sato, T., Igarashi, N., and Tanaka, N. (2002) The 2.0 angstrom crystal structure of catalase-peroxidase from *Haloarcula marismortui*. *Nat. Struct. Biol. 9*, 691–695.
3. Bertrand, T., Eady, N. A. J., Jones, J. N., Bodiguel, J., Jesmin, Nagy, J. M., Raven, E. L., Jamart-Gregoire, B., and Brown, K. H. (2004) Crystal structure of *Mycobacterium tuberculosis* catalase-peroxidase. *J. Biol. Chem. 279*, 38991–38999.
4. Ghiladi, R. A., Knudsen, G. M., Medzihradszky, K. F., and Ortiz de Montellano, P. R. (2005) The Met-Tyr-Trp cross link in *Mycobacterium tuberculosis* catalase peroxidase. *J. Biol. Chem. 280*, 22651–22663.
5. Carpena, X., Loprasert, S., Mongkolsuk, S., Switala, J., Loewen, P. C., and Fita, I. (2003) Catalase-peroxidase KatG of *Burkholderia pseudomallei* at 1.7 Å. *J. Mol. Biol. 327*, 475–489.
6. Jakopitsch, C., Ivancich, A., Schmuckenschlager, F., Wanasinghe, A., Poltl, G., Furtmuller, P. G., Ruker, F., and Obinger, C. (2004) Influence of the unusual covalent adduct on the kinetics and formation of radical intermediates in Synechocytic catalase peroxidase. *J. Biol. Chem. 279*, 46082–46095.
7. Jakopitsch, C., Auer, M., Ivancich, A., Ruker, F., Furtmuller, P. G., and Obinger, C. (2003) Total conversion of bifunctional catalase-peroxidase (KatG) to monofunctional peroxidase by exchange of a conserved distal side tyrosine. *J. Biol. Chem. 278*, 20185–20191.
8. Hillar, A., Peters, B., Pauls, R., Loboda, A., Zhang, H., Mauk, A. G., and Loewen, P. C. (2000) Modulation of the activities of catalase-peroxidase HPI of *Escherichia coli* by site-directed mutagenesis. *Biochemistry 39*, 5868–5875.
9. Ghiladi, R. A., Medzihradszky, K. F., and Ortiz de Montellano, P. R. (2005) Role of the Met-Tyr-Trp cross link in *Mycobacterium tuberculosis* catalase peroxidase (KatG) as revealed by KatG(M255I). *Biochemistry 44*, 15093–15105.
10. Pipirou, Z., Bottrill, A. R., Metcalfe, C. M., Mistry, S. C., Badyal, S. K., Rawlings, B. J., and Raven, E. L. (2007) Autocatalytic formation of a covalent link between tryptophan 41 and the heme in ascorbate peroxidase. *Biochemistry 46*, 2174–2180.
11. Scholes, C. P., Liu, Y., Fishel, L. A., Farnum, M. F., Mauro, J. M., and Kraut, J. (1989) Recent ENDOR and pulsed electron paramagnetic resonance studies of cytochrome *c* peroxidase Compound I and its site-directed mutants. *Isr. J. Chem. 29*, 85–92.
12. Sivaraja, M., Goodin, D. B., Smith, M., and Hoffman, B. M. (1989) Identification by ENDOR of Trp191 as the free-radical site in cytochrome *c* peroxidase Compound ES. *Science 245*, 738–740.
13. Fishel, L. A., Farnum, M. F., Mauro, J. M., Miller, M. A., Kraut, J., Liu, Y. J., Tan, X. L., and Scholes, C. P. (1991) Compound I radical in site-directed mutants of cytochrome *c* peroxidase as probed by electron paramagnetic resonance and electron-nuclear double resonance. *Biochemistry 30*, 1986–1996.
14. Erman, J. E., Vitello, L. B., Mauro, J. M., and Kraut, J. (1989) Detection of an oxy-ferryl porphyrin pi-cation radical in the reaction between hydrogen peroxide and a mutant yeast cytochrome *c* peroxidase. Evidence for tryptophan-191 involvement in the radical site of compound I. *Biochemistry 28*, 7992–7995.
15. Mauro, J. M., Fishel, L. A., Hazzard, J. T., Meyer, T. E., Tollin, G., Cusanovich, M. A., and Kraut, J. (1988) Tryptophan-191-phenylalanine, a proximal-side mutation in yeast cytochrome *c* peroxidase that strongly affects the kinetics of ferrocytochrome *c* oxidation. *Biochemistry 27*, 6243–6256.
16. Nelson, D. P., and Kiesow, L. A. (1972) Enthalpy of decomposition of hydrogen peroxide by catalase at 25 °C (with molar extinction coefficients of H_2O_2 solutions in the UV). *Anal. Biochem. 49*, 474–478.
17. Fishel, L. A., Villafranca, J. E., Mauro, J. M., and Kraut, J. (1987) Yeast cytochrome *c* peroxidase: Mutagenesis and expression in *Eschericia coli* show tryptophan-51 is not the radical site in compound I. *Biochemistry 26*, 351–360.
18. Murphy, E. J., Metcalfe, C. L., Basran, J., Moody, P. C., and Raven, E. L. (2008) Engineering the substrate specificity and reactivity of a heme protein: Creation of an ascorbate binding site in cytochrome *c* peroxidase. *Biochemistry 47*, 13933–13941.
19. Teale, F. W. (1959) Cleavage of the haem-protein link by acid methylethylketone. *Biochim. Biophys. Acta 35*, 543.
20. Friesner, R. A., and Guallar, V. (2005) Ab initio quantum chemical and mixed quantum mechanics/molecular mechanics (QM/MM) methods for studying enzymatic catalysis. *Annu. Rev. Phys. Chem. 56*, 389–427.
21. Senn, H. M., and Thiel, W. (2007) QM/MM methods for biological systems, in *Atomistic Approaches in Modern Biology: From Quantum Chemistry to Molecular Simulations* (Reiher, M., Ed.), pp 173−290, Springer, Berlin.
22. Jorgensen, W. L., Maxwell, D. S., and TiradoRives, J. (1996) Development and testing of the OPLS all-atom force field on conformational energetics and properties of organic liquids. *J. Am. Chem. Soc. 118*, 11225–11236.
23. Schrödinger, I. (2000) *IMPACT*, Portland, OR.
24. Schrödinger, I. (2001) *QSite*, Portland, OR.
25. Yonetani, T., and Ray, G. S. (1965) Studies on cytochrome *c* peroxidase. Purification and some properties. *J. Biol. Chem. 240*, 4503–4514.
26. Yonetani, T., Chance, B., and Kajiwara, S. (1966) Crystalline cytochrome *c* peroxidase and complex ES. *J. Biol. Chem. 241*, 2981–2982.
27. Coulson, A. F., and Yonetani, T. (1972) Oxidation of cytochrome c peroxidase with hydrogen peroxide: identification of the "endogenous donor". *Biochem. Biophys. Res. Commun. 49*, 391–398.
28. Miller, M. A., Vitello, L. B., and Erman, J. E. (1995) Regulation of interprotein electron transfer by Trp191 of cytochrome *c* peroxidase. *Biochemistry 34*, 12048–12058.
29. Hoffman, B. M., Roberts, J. E., Kang, C. H., and Margoliash, E. (1981) Electron paramagnetic and electron nuclear double resonance of the hydrogen peroxide compound of cytochrome *c* peroxidase. *J. Biol. Chem. 256*, 6556–6564.
30. Colas, C., Kuo, J. M., and Ortiz de Montellano, P. R. (2002) Asp-225 and glu-375 in autocatalytic attachment of the prosthetic heme group of lactoperoxidase. *J. Biol. Chem. 277*, 7191–7200.

31. Henne, K. R., Kunze, K. L., Zheng, Y.-M., Christmas, P., Soberman, R. J., and Rettie, A. E. (2001) Covalent linkage of prosthetic heme to CYP4 family of P450 enzymes. *Biochemistry 40*, 12925–12931.
32. Metcalfe, C. L., Ott, M., Patel, N., Singh, K., Mistry, S. C., Goff, H. M., and Raven, E. L. (2004) Autocatalytic formation of green heme: evidence for H_2O_2-dependent formation of a covalent methionine-heme linkage in ascorbate peroxidase. *J. Am. Chem. Soc. 126*, 16242–16248.
33. Limburg, J., LeBrun, L. A., and Ortiz de Montellano, P. R. (2005) The P450cam G248E mutant covalently binds its prosthetic heme group. *Biochemistry 44*, 4091–4099.
34. LeBrun, L. A., Xu, F., Kroetz, D. L., and Ortiz de Montellano, P. R. (2002) Covalent attachment of the heme prosthetic group in the CYP4 cytochrome P450 family. *Biochemistry 41*, 5931–5937.
35. Colas, C., and De Montellano, P. R. (2004) Horseradish peroxidase mutants that autocatalytically modify their prosthetic heme group: Insights into mammalian peroxidase heme-protein covalent bonds. *J. Biol. Chem. 279*, 24131–24140.
36. Svistunenko, D. A., Dunne, J., Fryer, M., Nicholls, P., Reeder, B. J., Wilson, M. T., Bigotti, M. G., Cutruzzola, F., and Cooper, C. E. (2002) Comparative study of tyrosine radicals in hemoglobin and myoglobins treated with hydrogen peroxide. *Biophys. J. 83*, 2845–2855.
37. Pipirou, Z., Bottrill, A. R., Svistunenko, D. A., Efimov, I., Basran, J., Mistry, S. C., Cooper, C. E., and Raven, E. L. (2007) The reactivity of heme in biological systems: Autocatalytic formation of both tyrosine-heme and tryptophan-heme covalent links in a single protein architecture. *Biochemistry 46*, 13269–13278.
38. Woo, T. K., Margl, P. M., Deng, L., Cavallo, L., and Ziegler, T. (1999) Towards more realistic computational modeling of homogenous catalysis by density functional theory: Combined QM/MM and ab initio molecular dynamics. *Catal. Today 50*, 479–500.
39. Guallar, V. (2008) Heme electron transfer in peroxidases: The propionate e-pathway. *J. Phys. Chem. B 112*, 13460–13464.
40. Guallar, V., and Olsen, B. (2006) The role of the heme propionates in heme biochemistry. *J. Inorg. Biochem. 100*, 755–760.
41. Cho, K. B., Derat, E., and Shaik, S. (2007) Compound I of nitric oxide synthase: the active site protonation state. *J. Am. Chem. Soc. 129*, 3182–3188.
42. Zheng, J., Wang, D., Thiel, W., and Shaik, S. (2006) QM/MM study of mechanisms for compound I formation in the catalytic cycle of cytochrome P450cam. *J. Am. Chem. Soc. 128*, 13204–13215.
43. Bathelt, C. M., Mulholland, A. J., and Harvey, J. N. (2005) QM/MM studies of the electronic structure of the compound I intermediate in cytochrome *c* peroxidase and ascorbate peroxidase. *Dalton Trans.* 3470–3476.
44. Zurek, J., Foloppe, N., Harvey, J. N., and Mulholland, A. J. (2006) Mechanisms of reaction in cytochrome P450: Hydroxylation of camphor in P450cam. *Org. Biomol. Chem. 4*, 3931–3937.
45. Beratan, D. N., and Balabin, I. A. (2008) Heme-copper oxidases use tunneling pathways. *Proc. Natl. Acad. Sci. U.S.A. 105*, 403–404.
46. Balabin, I. A., and Onuchic, J. N. (2000) Dynamically controlled protein tunneling paths in photosynthetic reaction centers. *Science 290*, 114–117.
47. Fox, T., Tsaprailis, G., and English, A. M. (1994) Fluorescence investigation of yeast cytochrome c peroxidase oxidation by H_2O_2 and enzyme activities of the oxidized enzyme. *Biochemistry 33*, 186–191.
48. Pfister, T. D., Gengenbach, A. J., Syn, S., and Lu, Y. (2001) The role of redox-active amino acids on compound I stability, substrate oxidation, and protein cross-linking in yeast cytochrome c peroxidase. *Biochemistry 40*, 14942–14951.
49. Ivancich, A., Dorlet, P., Goodin, D. B., and Un, S. (2001) Multifrequency high-field EPR study of the tryptophanyl and tyrosyl radical intermediates in wild-type and the W191G mutant of cytochrome *c* peroxidase. *J. Am. Chem. Soc. 123*, 5050–5058.
50. Tsaprailis, G., and English, A. M. (2003) Different pathways of radical translocation in yeast cytochrome *c* peroxidase and its W191F mutant on reaction with H_2O_2 suggest an antioxidant role. *J. Biol. Inorg. Chem. 8*, 248–255.
51. Zhang, H., He, S., and Mauk, A. G. (2002) Radical formation at Tyr39 and Tyr153 following reaction of yeast cytochrome *c* peroxidase with hydrogen peroxide. *Biochemistry 41*, 13507–13513.
52. Gengenbach, A., Syn, S., Wang, X., and Lu, Y. (1999) Redesign of cytochrome c peroxidase into a manganese peroxidase: Role of tryptophans in peroxidase activity. *Biochemistry 38*, 11425–11432.
53. Bhaskar, B., Immoos, C. E., Shimizu, H., Sulc, F., Farmer, P. J., and Poulos, T. L. (2003) A novel heme and peroxide-dependent tryptophan-tyrosine cross-link in a mutant of cytohrome *c* peroxidase. *J. Mol. Biol. 328*, 157–166.
54. Singh, R., Switala, J., Loewen, P. C., and Ivancich, A. (2007) Two [Fe(IV)═O Trp$^{\bullet}$] intermediates in *M. tuberculosis* catalase-peroxidase discriminated by multifrequency (9−285 GHz) EPR spectroscopy: Reactivity towards isoniazid. *J. Am. Chem. Soc. 129*, 15954–15963.

BI802210G